Contact-Invariant Total Energy Shaping Control for Powered Exoskeletons

Jianping Lin, Ge Lv, *Member, IEEE,* Robert D. Gregg, *Senior Member, IEEE*

***Abstract*— Energy shaping methods can be used to design task-invariant feedback control laws for the powered exoskeletons (i.e., orthoses). In order to achieve a desired closed-loop energy, certain matching conditions must be satisfied, which are sets of nonlinear partial differential equations. In this paper, we solve the matching conditions and come up with a new solution for under-actuated systems by using Auckly's method. We find a unified feedback control law that is task-invariant with respect to human inputs and different contact conditions. We propose assistive and resistive shaping strategies to alter the mass/inertia matrix and simulate on a powered knee-ankle exoskeleton. The simulation results show the reduction and increment of the human model's metabolic cost of generating muscular forces in human walking. The interchange between the kinetic and potential energy and the changes in acceleration of the center of mass are also investigated in the simulation.**

I. INTRODUCTION

Powered exoskeletons have been developed to serve as rehabilitation devices and provide gait assistance to human users. For example, the robot suit Hybrid Assistive Limb [1] enhances a healthy person's abilities and supports a physically challenged person's daily life. The control method utilized estimates a patient's intentions based on the ground reaction force. ReWalk [2] and Ekso Bionics [3] provide powered hip and knee motion to assist individuals with spinal cord injury (SCI) based on control technology with pre-defined reference trajectories determined by a finite-state machine. The bilateral Wandercraft exoskeleton [4] stabilizes walking gaits for users with SCI with control based on virtual constraints, hybrid zero dynamics, and gait optimization.

Although these exoskeletons show promising results in gait rehabilitation, significant challenges remain in their control strategies. The exoskeletons mentioned above use trajectory-based control methods, where the pre-defined trajectories cannot adjust to continuously varying activities and thus limit their overall adaptability. In contrast, task-invariant control for powered exoskeletons provides more flexibility in assisting humans in a continuum of activities despite the specific tasks and environment changes. For example, Lv et al. [5], [6], [7] proposed task-invariant controllers for the powered exoskeletons using energy shaping methods. Energy shaping methods [8] alter the dynamic characteristics of a mechanical system via the Euler-Lagrange equations and have already seen success in applications of bipedal locomotion. Bloch et al. [9] proposed the controlled Lagrangians method where the Lagrangian defined by the difference of the kinetic energy and potential energy of the system is mapped to a suitable closed-loop Euler-Lagrange system. Spong [10] proposed the method of controlled symmetries that reproduces passive limit cycles on arbitrary slopes.

The application of the energy shaping method must satisfy a set of nonlinear partial differential equations (PDEs called the matching conditions), which are generally difficult to solve. However, Auckley et al. [11] proposed a method which converts the nonlinear PDEs to a set of linear PDEs, which are easier to solve. Blankenstein et al. [12] summarized the discussion of the matching conditions and applied these methods to the general class of under-actuated mechanical systems. Holm et al. [13] solved the matching conditions and achieved walking speed regulation through the under-actuated control law arising from shaping the kinetic energy of a bipedal robot. However, the model used in [13] was a compass-gait bipedal robot with only 2 degrees of freedom (DOFs) and actuators at the ankles. Environmental interaction or more complex human-exoskeleton dynamics were not considered.

In this paper, we consider the matching condition with a higher DOF system compared to the system in [13]. By using the conversion method in [11], we find a new solution of the matching conditions. This new solution includes the particular solutions derived in [6], [13] and specifies the feasible shaping structure of dynamic terms in the closed-loop system. Prior work [6], [7] only shaped the mass and lower-limb inertias in the actuated part of the mass matrix. Moreover, the control law in [6] was derived from equivalent constrained dynamics and changed with different contact conditions. In this paper, we propose a unified control law across contact conditions that shapes both actuated and unactuated parts of the inertia matrix. This unified control law does not depend on particular tasks or subjects. We investigate the change of metabolic cost, the interchange of kinetic and potential energy, and the acceleration of the center of mass (COM) based on the mass/inertia matrix in the closed-loop system.

The rest of this paper is organized as follows. In Section II, we review the concepts of the controlled Lagrangians method [9] and the techniques of Auckly et al. [11]. Based on these techniques, we find a new solution of the matching conditions. The dynamics of a human-like biped are shown in Section III with consideration of contact conditions. We then

Asterisk indicates the corresponding author.

J. Lin and R. D. Gregg* are with the Departments of Bioengineering and Mechanical Engineering, University of Texas at Dallas, Richardson, TX 75080, USA. rgregg@ieee.org

G. Lv is with the Robotics Institute, Carnegie Mellon University, Pittsburgh, PA 15213, USA.

This work was supported by NSF Award CMMI-1652514. R. D. Gregg holds a Career Award at the Scientific Interface from the Burroughs Wellcome Fund and the Eugene McDermott Professorship of UT Dallas.

design the unified control law across contact conditions and show two types of total energy shaping strategies. Simulation results are given in Section IV. Finally, Section V presents the conclusion.

II. The Matching Condition

In this section, we review the definition of energy shaping and the converting method of Auckly et al. [11] for the matching conditions. After that, we derive a new solution of the matching conditions, which is a generalization of the solutions in [6], [13].

A. Review of General Matching Conditions

Considering a forced Euler-Lagrange system with n-dimensional configuration space Q, the corresponding Lagrangian $L(q,\dot{q}):\ TQ \to \mathbb{R}$ has the form

$$L(q,\dot{q}) = K(q,\dot{q}) - V(q) = \frac{1}{2}\dot{q}^T M(q)\dot{q} - V(q),$$

where $K(q,\dot{q})$ is the kinetic energy based on the generalized mass/inertia matrix $M(q)$, and $V(q)$ is the potential energy. The dynamics of $L(q,\dot{q})$ are given as

$$\frac{\mathrm{d}}{\mathrm{dt}}\partial_{\dot{q}}L(q,\dot{q}) - \partial_q L(q,\dot{q}) = B(q)u, \tag{1}$$

where $u \in \mathbb{R}^r$ is the control input and $B \in \mathbb{R}^{n\times r}$ maps the inputs u to the Euler-Lagrange system with $rank(B) = r$. We can factor equation (1) into the common form as

$$M(q)\ddot{q} + C(q,\dot{q})\dot{q} + N(q) = B(q)u, \tag{2}$$

where $C(q,\dot{q})$ is the Coriolis matrix, and $N(q)$ is the gradient of the potential energy $V(q)$ along the generalized coordinates.

Consider the closed-loop Lagrangian system

$$\frac{\mathrm{d}}{\mathrm{dt}}\partial_{\dot{q}}\tilde{L}(q,\dot{q}) - \partial_q\tilde{L}(q,\dot{q}) = 0,$$

which can be represented as

$$\tilde{M}(q)\ddot{q} + \tilde{C}(q,\dot{q})\dot{q} + \tilde{N}(q) = 0 \tag{3}$$

with the modified dynamic terms $\tilde{M}(q)$, $\tilde{C}(q,\dot{q})$, and $\tilde{N}(q)$. The suitable control law u relating the closed-loop system to the open-loop system must satisfy

$$\begin{aligned} Bu &= \frac{\mathrm{d}}{\mathrm{dt}}(\partial_{\dot{q}}L) - \partial_q L - \frac{\mathrm{d}}{\mathrm{dt}}(\partial_{\dot{q}}\tilde{L}) + \partial_q\tilde{L} \\ &= M\ddot{q} + C\dot{q} + N - \tilde{M}\ddot{q} - \tilde{C}\dot{q} - \tilde{N}, \end{aligned} \tag{4}$$

where we omit the arguments q and $\dot{q}$ of the dynamic terms to abbreviate notation. Substituting $\ddot{q} = -\tilde{M}^{-1}(\tilde{C}\dot{q} + \tilde{N})$ in equation (4), we have

$$Bu = M[M^{-1}(C\dot{q} + N) - \tilde{M}^{-1}(\tilde{C}\dot{q} + \tilde{N})].$$

According to [12], systems (2) and (3) match if and only if there exists a full rank left annihilator of $B(q)$, i.e., $B^{\perp}(q)B(q) = 0$, for all $q \in Q$ such that

$$B^{\perp}M[M^{-1}(C\dot{q} + N) - \tilde{M}^{-1}(\tilde{C}\dot{q} + \tilde{N})] = 0 \tag{5}$$

holds true, where the corresponding state feedback control law is explicitly given by

$$u = (B^T B)^{-1}B^T M[M^{-1}(C\dot{q} + N) - \tilde{M}^{-1}(\tilde{C}\dot{q} + \tilde{N})].$$

Utilizing the fact that $C\dot{q} = D_q(M\dot{q})\dot{q} - \frac{1}{2}\nabla_q^T(\dot{q}^T M\dot{q})$ and $N = \nabla_q V$ [14], we can rewrite equation (5) as

$$\begin{aligned} B^{\perp}M[M^{-1}(D_q(M\dot{q})\dot{q} - \frac{1}{2}\nabla_q^T(\dot{q}^T M\dot{q}) + \nabla_q V) - \\ \tilde{M}^{-1}(D_q(\tilde{M}\dot{q})\dot{q} - \frac{1}{2}\nabla_q^T(\dot{q}^T\tilde{M}\dot{q}) + \nabla_q\tilde{V})] = 0, \end{aligned} \tag{6}$$

where $\tilde{N} = \nabla_q\tilde{V}$. The matching condition is a complicated nonlinear PDE in two unknowns $\tilde{M}$ and $\tilde{V}$, which is difficult to solve [9]. To simplify solving for the matching condition, Auckly et al. proposed a method to solve equation (6) by recursively solving a set of three linear PDEs in [11]. As summarized in [12] and [13], we have the first equation, for all vector fields $X \in T_qQ$ at some points $q \in Q$,

$$\begin{aligned} 0 = X^T M\bar{B}^{\perp}\Lambda^T[\partial_q(M\bar{B}^{\perp}MX) - \partial_q(\bar{B}^{\perp}MX)M \\ + 2M\partial_q(\bar{B}^{\perp}MX)] - X^T M\bar{B}^{\perp}[\partial_q(M\Lambda\bar{B}^{\perp}MX) \\ - \partial_q(\Lambda\bar{B}^{\perp}MX)M + 2M\partial_q(\Lambda\bar{B}^{\perp}MX)], \end{aligned} \tag{7}$$

where $\Lambda = \tilde{M}^{-1}M$ and matrix $\bar{B}^{\perp}$ denotes the left annihilator of B in the orthogonal projection form, i.e., $(\bar{B}^{\perp})^T = \bar{B}^{\perp}$ and $(\bar{B}^{\perp})^2 = \bar{B}^{\perp}$. The second equation is given as

$$\begin{aligned} 0 = M\bar{B}^{\perp}\Lambda^T[\partial_q(\frac{1}{2}\dot{q}^T\tilde{M}\dot{q}) - \partial_q(\tilde{M}\dot{q})\dot{q}] \\ + M\bar{B}^{\perp}[-\partial_q(\frac{1}{2}\dot{q}^T M\dot{q}) + \partial_q(M\dot{q})\dot{q}],\ \forall(q,\dot{q}) \in TQ. \end{aligned} \tag{8}$$

Finally, the third equation, which gives the solution of the closed-loop potential energy, is given as

$$0 = M\bar{B}^{\perp}\partial_q V - M\bar{B}^{\perp}\Lambda^T\partial_q\tilde{V}. \tag{9}$$

It is shown in [11], [15] that the solution of the matching condition (6) can be obtained by solving these three linear PDEs, i.e., (7) to (9). We first solve (7) for the unknown $\Lambda\bar{B}^{\perp}M$ and plug it back into (8), which now is a linear PDE in $\tilde{M}$. Finally, with a feasible solution of $\tilde{M}$, solving (9) will thus give the solution for the potential energy $\tilde{V}$.

B. Solving PDEs with Specific $B(q)$

Consider the mapping matrix $B(q) = [0_{r\times(n-r)}, I_{r\times r}]^T$, the corresponding orthogonal projection matrix is given as

$$\bar{B}^{\perp} = \begin{bmatrix} I_{(n-r)\times(n-r)} & 0_{(n-r)\times r} \\ 0_{r\times(n-r)} & 0_{r\times r} \end{bmatrix}.$$

Based on the orthogonal projection matrix $\bar{B}^{\perp}$, we find a new solution to the linear PDEs (7) to (9) by setting

$$\Lambda\bar{B}^{\perp}M = \frac{1}{k_1}\bar{B}^{\perp}M, \tag{10}$$

which is multiplied by a constant value $\frac{1}{k_1}$. The fact that matching condition (7) holds true can be easily verified by

plugging (10) into it. In order for matching condition (8) to hold true, we need to have

$$0 = M\bar{B}^{\perp} f(q,\dot{q}) = M \begin{bmatrix} f_{1:(n-r)} \\ 0_{r\times 1} \end{bmatrix}, \tag{11}$$

where $f(q,\dot{q}) := \frac{1}{k_1}[\partial_q(\frac{1}{2}\dot{q}^T\tilde{M}\dot{q}) - \partial_q(\tilde{M}\dot{q})\dot{q}] - \partial_q(\frac{1}{2}\dot{q}^T M\dot{q}) + \partial_q(M\dot{q})\dot{q} \in \mathbb{R}^{n\times 1}$ and we denote $f_{1:(n-r)} = [f_1,\cdots,f_{n-r}]^T$ to be the first $n-r$ rows of vector f for simplicity. The k-th row of vector f is given as

$$f_k = \sum_{i=1}^{n}\sum_{j=1}^{n} \dot{q}_i\left(\frac{\partial M_{kj}}{\partial q_i} - \frac{1}{k_1}\frac{\partial \tilde{M}_{kj}}{\partial q_i} - \frac{1}{2}\frac{\partial M_{ij}}{\partial q_k} + \frac{1}{2k_1}\frac{\partial \tilde{M}_{ij}}{\partial q_k}\right)\dot{q}_j.$$

Since M is positive definite, (11) is equivalent to $f_{1:(n-r)} = 0$ holding true along all trajectories $(q,\dot{q}) \in TQ$. As a result, for $k \in \{1,\ldots,(n-r)\}$ and $(i,\ j) \in \{1,\ldots,(n-r)\}$, we have

$$\frac{\partial M_{kj}}{\partial q_i} - \frac{1}{k_1}\frac{\partial \tilde{M}_{kj}}{\partial q_i} - \frac{1}{2}\frac{\partial M_{ij}}{\partial q_k} + \frac{1}{2k_1}\frac{\partial \tilde{M}_{ij}}{\partial q_k} = 0.$$

The new solution of $\tilde{M}$ is then given by

$$\tilde{M}_{ij} = k_1 M_{ij},\ \forall (i,\ j) \in \{1,\ldots,(n-r)\}.$$

For $k \in \{1,\ldots,(n-r)\}$ and $(i,\ j) \in \{(n-r+1),\ldots,n\}$, we can simplify $f_k = 0$ as

$$-\frac{1}{2}\frac{\partial M_{ij}}{\partial q_k} + \frac{1}{2}\frac{\partial \tilde{M}_{ij}}{\partial q_k} = \frac{1}{2}\frac{\partial \tilde{M}_{ij}}{\partial q_k} = 0,$$

where $\frac{\partial M_{ij}}{\partial q_k} = 0$ due to the recursively cyclic property of q_k as shown in [6]. The new solution of $\tilde{M}$ must satisfy that

$$\tilde{M}_{ij} = \tilde{M}_{ij}(q_{(n-r+1):n}),\ \forall (i,\ j) \in \{(n-r+1),\ldots,n\},$$

i.e., $\tilde{M}_{ij}$ is independent of $q_{1:(n-r)}$. By plugging (10) into (9), we have

$$\begin{aligned} 0 &= M\bar{B}^{\perp}[\partial_q V - \frac{1}{k_1}\partial_q \tilde{V}] = M\bar{B}^{\perp}[N - \frac{1}{k_1}\tilde{N}] \\ &= M\begin{bmatrix} N_{1:(n-r)} - \frac{1}{k_1}\tilde{N}_{1:(n-r)} \\ 0_{r\times 1} \end{bmatrix}. \end{aligned}$$

As a consequence, the closed-loop gravitational force vector is given as $\tilde{N} = [k_1 N^T_{1:(n-r)}, \tilde{N}^T_{(n-r+1):n}]^T$.

Additionally, because $\Lambda = \tilde{M}^{-1}M$, we must have

$$\Lambda\bar{B}^{\perp}M = \frac{1}{k_1}\bar{B}^{\perp}M = \tilde{M}^{-1}M\bar{B}^{\perp}M. \tag{12}$$

To show this additional condition (12) is also satisfied with the new solution, we can decompose the mass/inertia matrix M into M_1, M_2, and M_4 and define $\tilde{M}$ based on the decomposition of M as

$$M = \begin{bmatrix} M_1 & M_2 \\ M_2^T & M_4 \end{bmatrix},\ \tilde{M} = \begin{bmatrix} k_1 M_1 & k_1 M_2 \\ k_1 M_2^T & \tilde{M}_4 \end{bmatrix}, \tag{13}$$

where $M_1 \in \mathbb{R}^{(n-r)\times(n-r)}$, $M_2 \in \mathbb{R}^{(n-r)\times r}$, and $M_4, \tilde{M}_4 \in \mathbb{R}^{r\times r}$ with $q_{1:(n-r)}$ being cyclic in M_4 and $\tilde{M}_4$ [16]. As a result, we can calculate $\tilde{M}^{-1}M$ as

$$\tilde{M}^{-1}M = \begin{bmatrix} \frac{1}{k_1}I & \Sigma_1 \\ 0 & \Sigma_2 \end{bmatrix},$$

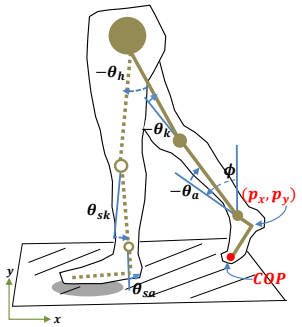

Fig. 1. Kinematic model of the human body. COP denotes the Center of Pressure. The solid links denote the stance leg, the dashed links denote the swing leg. This figure is reproduced from [17].

where

$$\tilde{\Delta} = k_1(M_1 - k_1 M_2 \tilde{M}_4^{-1} M_2^T),\ \Sigma_1 = \tilde{\Delta}^{-T} M_2 (I - k_1 \tilde{M}_4{}^{-1} M_4),$$
$$\Sigma_2 = k_1 \tilde{M}_4^{-1} M_2^T \tilde{\Delta}^{-T} M_2 (k_1 \tilde{M}_4^{-1} M_4 - I) + \tilde{M}_4^{-1} M_4.$$

By plugging $\tilde{M}^{-1}M$ into (12) and with the specific $\bar{B}^{\perp}$, the additional condition (12) is also satisfied with the new solution.

III. Biped Control Application

In this section, we first review the dynamics of the biped that will be used for simulating the proposed control approach. We then design a unified control law that is task-invariant with respect to human inputs and different contact conditions. Finally, we propose two types of shaping strategies to alter the structure of dynamic terms.

A. Review of Dynamics of the Biped

The biped model with coupled dynamics of the two legs is shown in Fig. 1. We combine the masses of the human limb and the exoskeleton together in the model. We assume that we have identical powered knee-ankle exoskeletons on both human legs with no connection between them to avoid asymmetric gaits in simulation [7], [18]. For deriving controllers that only require local feedback, we separate the dynamical models of the stance and swing legs, which are coupled through interaction forces.

Consider the generalized Lagrangian dynamics of the biped with contact constraints as

$$M\ddot{q} + C\dot{q} + N + A_l^T \lambda = \tau. \tag{14}$$

We denote the human and exoskeleton torques as $\tau = \tau_{exo} + \tau_{hum} = Bu + Bv + J^T F$ where $B \in \mathbb{R}^{n\times r}$ maps the human and exoskeleton inputs into the dynamics and we assume $B = [0_{r\times(n-r)}, I_{r\times r}]^T$. The control input $u \in \mathbb{R}^{r\times 1}$ consists of the torques provided by exoskeleton and $v \in \mathbb{R}^{r\times 1}$ represents the human input. The interaction forces between the hip and the swing thigh are represented by F and mapped to the system by the body Jacobian matrix J. The Lagrange

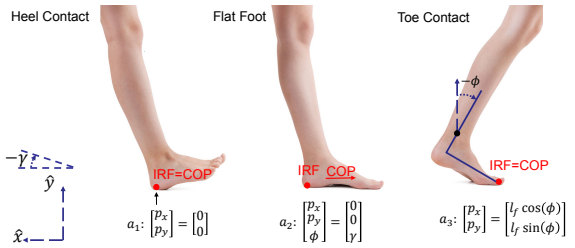

Fig. 2. Heel contact (left), flat foot (center), and toe contact conditions (right) during the single-support period of human locomotion. The biped is assumed to be walking on a slope with angle γ. This figure is reproduced from [7].

multiplier $\lambda \in \mathbb{R}^{c\times 1}$ represents the ground reaction forces and can be calculated as [14], [19]

$$\lambda = (A_l M^{-1} A_l^T)^{-1}[A_l M^{-1}(\tau - C\dot{q} - N) + \dot{A}_l \dot{q}].$$

The holonomic contact constraints of the biped can be expressed as $a_l(q) = 0_{c\times 1}$ where c denotes the number of constraints. The constraint matrix $A_l = \nabla_q a_l \in \mathbb{R}^{c\times n}$ satisfies $A_l(q)\dot{q} = 0$ and can be represented by $A_l = [A_1\ A_2]$ with the invertible matrix $A_1 \in \mathbb{R}^{c\times c}$ and $A_2 \in \mathbb{R}^{c\times(n-c)}$. The subscript $l \in \{heel, flat, toe\}$ indicates the contact configurations as shown in Fig. 2.

B. Unified Control Law with Contact Constraints

Our goal is to design a task-invariant feedback control law for the powered exoskeleton where the control law does not depend on different contact conditions or the human input. Given the open-loop dynamics (14), based on Section II-B, we wish to achieve the closed-loop dynamics as

$$\tilde{M}\ddot{q} + \tilde{C}\dot{q} + \tilde{N} + \tilde{A}_l^T \lambda = \tilde{B}v + \tilde{J}^T F,$$

where $\tilde{M}$ is given in (13), $\tilde{C}$ is based on $\tilde{M}$, and $\tilde{N} = [k_1 N_{1:(n-r)}^T,\ N_{(n-r+1):n}^T]^T$. The corresponding control law is

$$\begin{aligned} u = (B^T B)^{-1} B^T M [M^{-1}(C\dot{q} + N + A_l^T \lambda - Bv - J^T F) \\ - \tilde{M}^{-1}(\tilde{C}\dot{q} + \tilde{N} + \tilde{A}_l^T \lambda - \tilde{B}v - \tilde{J}^T F)]. \end{aligned}$$

In general, the human joint input v and the interaction forces F are difficult to measure in practice. As a result, we set $\tilde{B} = \tilde{M}M^{-1}B$ and $\tilde{J}^T = \tilde{M}M^{-1}J^T$, so that the human input and the interaction forces disappear in the matching condition (5) and the control law is invariant with respect to the human inputs. We also treat the ground reaction forces $\tilde{A}_l^T \lambda$ as the external forces and assume that $\tilde{A}_l^T = \tilde{M}M^{-1}A_l^T$ which makes the corresponding control law independent of the ground reaction forces. Therefore, the control law is unified with respect to different contact conditions. The corresponding control law is then

$$u = (B^T B)^{-1} B^T [(C\dot{q} - M\tilde{M}^{-1}\tilde{C}\dot{q}) + (N - M\tilde{M}^{-1}\tilde{N})]. \quad (15)$$

C. Shaping Strategies

Based on the way we define $\tilde{M}$ and $\tilde{N}$, we propose two types of different shaping strategies as case studies, where the first one scales the mass/inertia matrix with proper factors to ensure the positive definiteness of the mass/inertia matrix, and the second one adds an additional component to the scaled mass/inertia matrix.

1) Scaling Mass/Inertia Matrix: Based on the matching condition, we can define the mass/inertia matrix and the potential energy as

$$\tilde{M} = k_1 M,\ \tilde{N} = [k_1 N_{1:(n-r)}^T,\ N_{(n-r+1):n}^T]^T,\ \tilde{C} = k_1 C.$$

By plugging $\tilde{M}$, $\tilde{C}$, and $\tilde{N}$ into the control law (15), we obtain a control law that is equivalent to the potential energy (PE) shaping in [5] as $u = (B^T B)^{-1} B^T (N - \frac{1}{k_1}\tilde{N})$. The scaling factor k_1 modifies the gravitational forces along $q_{(n-r+1):n}$. With $k_1 > 1$ or $k_1 < 1$, we can have assistive or resistive torques from the exoskeleton, respectively.

2) Modified Mass/Inertia Matrix: Based on [13], we can add an additional term to the fully-actuated part of the mass/inertia matrix to alter the biped's gait characteristics where

$$\tilde{M} = k_1 \begin{bmatrix} M_1 & M_2 \\ M_2^T & M_4 + H \end{bmatrix},\ \tilde{N} = [k_1 N_{1:(n-r)}^T,\ N_{(n-r+1):n}^T]^T,$$

$$\tilde{C}\dot{q} = k_1 C\dot{q} + k_1 \begin{bmatrix} 0 & 0 \\ 0^T & \dot{H}\dot{q}_e - \frac{1}{2}\nabla_{q_e}^T(\dot{q}_e^T H \dot{q}_e) \end{bmatrix},$$

where $q_e = q_{(n-r+1):n}$, and $H \in \mathbb{R}^{r\times r}$ does not depend on $q_{1:(n-r)}$. The matching conditions (7) to (9) can be easily verified, while for $\tilde{M}$ to be positive definite, we need to have $k_1[(M_4 + H) - M_2^T M_1^{-1} M_2] > 0$ by using the Schur complement [20]. To satisfy this, we set H to be

$$H = \begin{bmatrix} 0_{(r-1)\times(r-1)} & 0_{(r-1)\times 1} \\ 0_{1\times(r-1)} & h \end{bmatrix},$$

where $h \in \mathbb{R}^1$ and will be specified in Section IV. By setting $\Omega = M/M_1 = M_4 - M_2^T M_1^{-1} M_2$ with M/M_1 representing the Schur complement of M, we can decompose Ω into four submatrices as

$$\Omega = \begin{bmatrix} \Omega_1 & \Omega_2 \\ \Omega_2^T & \Omega_4 \end{bmatrix},$$

where $\Omega_1 \in \mathbb{R}^{(r-1)\times(r-1)}$ and $\Omega_4 \in \mathbb{R}^1$. For $H + \Omega = H + M_4 - M_2^T M_1^{-1} M_2$ to be positive definite, we must have $\Omega/\Omega_1 + h > 0$, where $\Omega/\Omega_1 = \Omega_4 - \Omega_2^T \Omega^{-1} \Omega_2$ represents the Schur complement of Ω. To ensure the positive definiteness of $\tilde{M}$, we need to have $h > \lfloor -\Omega/\Omega_1 \rfloor$ with $\lfloor \cdot \rfloor$ representing the lower-bound.

IV. Simulations and Results

In this section, we demonstrate simulation results on an 8-DOF human-like biped to investigate the assistive and resistive effects of the proposed control strategies. The coupled dynamics of the two legs are shown in Fig. 1. The configuration space of the full biped model is given as $q = (p_x, p_y, \phi, \theta_a, \theta_k, \theta_h, \theta_{sk}, \theta_{sa})^T \in \mathbb{R}^{8\times 1}$, where (p_x, p_y) are the Cartesian coordinates of the heel with respect to the inertial reference frame (IRF), ϕ is the angle of the heel with respect to the vertical axis, θ_a and θ_k are the stance ankle and knee angles, respectively, θ_h represents the hip angle between the stance and swing thighs, θ_{sk} and θ_{sa} are the swing knee and ankle angles, respectively.

A. Simulation Model and Hybrid Dynamics

As mentioned in Section III, we assume that we have identical powered knee-ankle exoskeletons on both human legs. As a result, the corresponding controllers (15) for both legs only require local feedback.

For the dynamical model of the stance leg, the configuration vector is given as $q_{st} = (p_x, p_y, \phi, \theta_a, \theta_k)^T \in \mathbb{R}^{5\times 1}$. As shown in Fig. 2, the stance period can be divided into three phases [5]. The IRF is defined at the heel during the heel contact and the flat foot conditions. For the heel contact phase, the heel is fixed to the ground and the stance leg rotates around the heel. The holonomic contact constraint is $a_{heel}(q_{st}) = (p_x, p_y)^T = 0$ and the matrix $A_{heel} = \nabla_{q_{st}} a_{heel} = [I_{2\times 2}, 0_{2\times 3}]^T$. At the flat foot phase, the foot is flat on the ground slope and ϕ is equal to the slope angle γ. The constraint is $a_{flat}(q_{st}) = (p_x, p_y, \phi - \gamma)^T = 0$ and the matrix $A_{flat} = [I_{3\times 3}, 0_{3\times 2}]^T$. During the toe contact phase, the stance leg rotates around the toe and the IRF shifts instantly from the heel to the toe as described in [5]. The corresponding constraint is $a_{toe}(q_{st}) = (p_x - l_f \cos(\phi), p_y - l_f \sin(\phi))^T = 0$ and the matrix A_{toe} is given as

$$A_{toe}(q_{st}) = \begin{bmatrix} 1 & 0 & l_f \sin(\phi) & 0 & 0 \\ 0 & 1 & -l_f \cos(\phi) & 0 & 0 \end{bmatrix}.$$

For the dynamical model of the swing leg, the configuration vector is given as $q_{sw} = (h_x, h_y, \theta_{th}, \theta_{sk}, \theta_{sa})^T \in \mathbb{R}^{5\times 1}$, where (h_x, h_y) are the positions of the hip with respect to the IRF, and θ_{th} is the angle between the vertical axis and the swing thigh. We do not have contact constraints in the swing leg dynamics, i.e., $A(q_{sw}) = 0$.

The full biped is modeled as a hybrid dynamical system similar in [7], [18], where impacts happen at the change of contact conditions. The orbital stability of the hybrid dynamics are checked by Poincaré section methods as shown in [7]. We simulate the effect of different shaping strategies on a passive, downslope walking gait, which we generate using joint impedance control for the human inputs [21]. The simulated human inputs are assumed to be $v = -K_p e - K_d \dot{e}$, where $e = q_e - \bar{q}_e$ represents the difference between the actuated coordinates q_e and the fixed equilibria vector $\bar{q}_e$. The human impedance parameters K_p and K_d are chosen from Table I in [7] and kept constant with respect to each phase of stance to achieve the stable limit cycle of the biped.

B. Simulation Methods

We plug in different parameters of k_1 and k_2 into the control law (15) and simulate them accordingly to study their possible benefits on biped walking. The number of actuators $r = 2$ consists of the ankle and knee joints from the exoskeleton. Considering the case of total energy shaping with a scaling mass/inertia matrix, we found that the scaling factor k_1 should be within $[0.87, 1.18]$ so that the biped can walk downslope without falling due to excessive or insufficient energy in the simulation.

For the total energy shaping with a modified mass/inertia matrix, as mentioned in [22], the kinetic energy and potential energy interchange during biped walking. Convergence toward the limit cycle on a given slope requires dissipating energy upon ground impact at the end of each step [17]. Motivated by this fact, the additive term h is set to be $h(\theta_h) < 0$ for any $\theta_h \neq 0$, and $h(\theta_h) = 0$ with $\theta_h = 0$, so that the closed-loop system dissipates energy near the beginning and the end of each step. We choose $h(\theta_h) = k_2 \cdot (\theta_h)^2$ in the simulation with the assumption that $\theta_h \in [-\frac{\pi}{2}, \frac{\pi}{2}]$, so that $k_2 > -0.15 \approx -4\frac{|\Omega/\Omega_1|}{\pi^2} \geq -\frac{|\Omega/\Omega_1|}{(\theta_h)^2}$ ensures the positive definiteness of $\tilde{M}$. With the help of the additional term h in the knee actuator, the range of the scaling factor k_1 is enlarged to $[0.8, 1.33]$. As a result, the change of the gravitational forces along the actuated joints can be enhanced. For the swing leg, we only simulate the shaping strategy with scaling factor k_1.

In this paper, we propose two types of shaping strategies to provide assistance and resistance during walking. Strategies 1_{Ass} and 1_{Res} are based on the shaping method with the scaling mass/inertia matrix (i.e., PE shaping), whereas, strategies 2_{Ass} and 2_{Res} are based on the shaping method with the modified mass/inertia matrix. The choices of k_1 and k_2 are summarized in Table I.

TABLE I
CHOICES OF k_1 AND k_2 FOR DIFFERENT SHAPING STRATEGIES.

	1_{Ass}	1_{Res}	2_{Ass}	2_{Res}
k_1	1.18	0.87	1.33	0.8
k_2			-0.05	-0.05

C. Results and Discussion

The exoskeleton torques during one steady step are shown in Fig. 3. The type of shaping strategies with the modified mass/inertia matrix provides larger torques than the type of shaping strategies with the scaling mass/inertia matrix. In late stance, the scaling mass/inertia matrix generates knee flexion torque that lifts the lower-limb for the upcoming swing phase. The modified mass/inertia matrix changes the signs of the torques for the knee joint and generates knee extension torques to propel the body upwards and forwards which matches with the real human knee torque [23].

Fig. 4 gives the simulated human metabolic costs for different shaping strategies, where the metabolic cost defined in [24] is given as

$$\alpha_j^2 = \frac{\int_0^T v_j^2(t)\mathrm{d}t}{T(mgl)^2} \approx \frac{\sum_{i=1}^{N_T} v_j^2(i)\Delta t(i)}{T(mgl)^2}.$$

The term T is the step time period, N_T is the number of time steps in the simulation, v_j is the human joint moment, m is the overall mass of the biped, and l is the length of the biped's leg. The metabolic costs compute the sum of the costs of all human joints over one step, which can reflect the energy consumption of muscles that generate forces. As shown in Fig. 4, shaping strategies 1_{Ass} and 2_{Ass} reduce the metabolic cost given $k_1 > 1$, and strategies 1_{Res} and 2_{Res} increase the metabolic cost given $k_1 < 1$. Meanwhile, the modification on the actuated part of the mass/inertia matrix enlarges the range of the scaling factor, which results in an enhancement of the change of the metabolic cost. Strategies

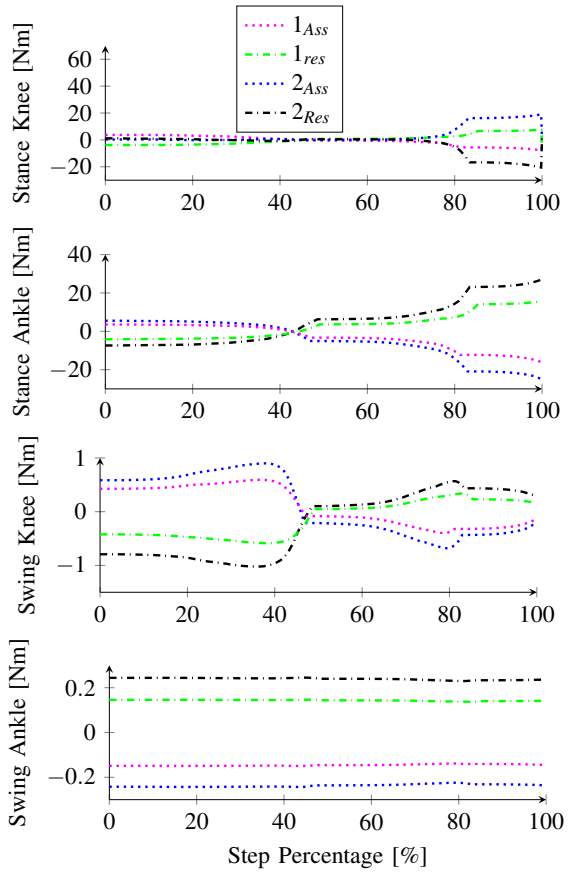

Fig. 3. The exoskeleton torque with different shaping strategies during one steady step. The cases with the modified mass/inertia matrix provide larger assistive/resistive torques.

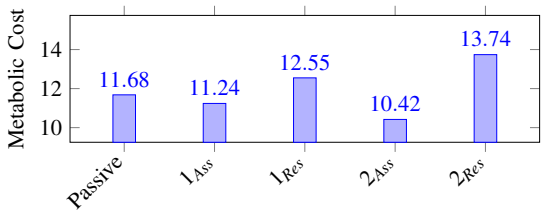

Fig. 4. The estimated metabolic costs with different shaping strategies. Strategies 2_{Ass} and 2_{Res} result in larger reduction and increase in the metabolic cost, respectively.

2_{Ass} and 2_{Res} create larger changes in metabolic cost than strategies 1_{Ass} and 1_{Res}.

Based on [25], the COM of the body is lowered during the forward acceleration and raised during the forward deceleration during level-ground walking. Consequently, the change of kinetic energy is transformed into an increase of potential energy, i.e., $\Delta PE = mgS_V$ with m representing the mass of the body and S_V representing the vertical displacement of the COM within each step. The mechanical energy is largely conserved during walking by the interchange between the kinetic energy and the gravitational potential energy [26]. Even with the work done by the control forces, the modification of the mechanical energy of the system is exactly

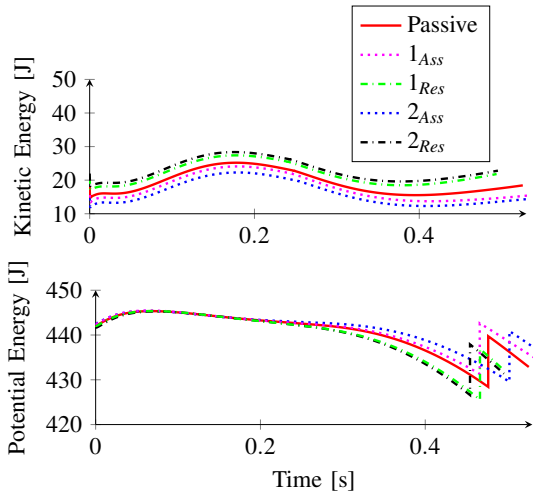

Fig. 5. Kinetic and potential energy during one steady step. The instantaneous jump in the potential energy in late stance corresponds to the shift of IRF from heel to toe during the toe contact configuration.

conserved by the closed-loop dynamics [27], [28]. Fig. 5 shows the interchange between the kinetic and potential energy where the scaling factor affects the transfer of kinetic energy to potential energy. With $k_1 > 1$, the variation of the potential energy is decreased, which yields a smaller vertical displacement of the COM and as a result, the metabolic cost is reduced according to [29]. With the help of the additional term on the actuated part of the mass/inertia matrix, we can further affect the interchange between the kinetic and potential energy.

As shown in [30], the force generated to support body weight and the work performed to redirect and accelerate the COM comprises a large part of metabolic cost during normal walking. As a result, we investigate the acceleration of the COM in the simulation. The acceleration of the COM along horizontal (x) and vertical (y) directions are shown in Fig. 6 and exhibit mostly negative/positive values for the horizontal/vertical directions due to the passive, downslope walking gait in the simulation. For the cases of total energy shaping with the scaling mass/inertia matrix, we have more advantages on the acceleration of COM along vertical direction, while the total energy shaping with the modified mass/inertia matrix helps during the forward and backward accelerations.

V. CONCLUSIONS

In this paper, we applied the energy shaping method to design a feedback control law for the powered exoskeleton that is invariant with respect to the human inputs and the different contact conditions. The energy shaping method maps the Euler-Lagrange dynamics to a desired closed-loop form through the feedback control law. In order for this feedback control law to exist, certain matching conditions should be satisfied, which are described by a set of nonlinear PDEs. Based on Auckly's method [11], we solved the matching conditions and obtained a new solution for under-actuated systems. We proposed two types of shaping

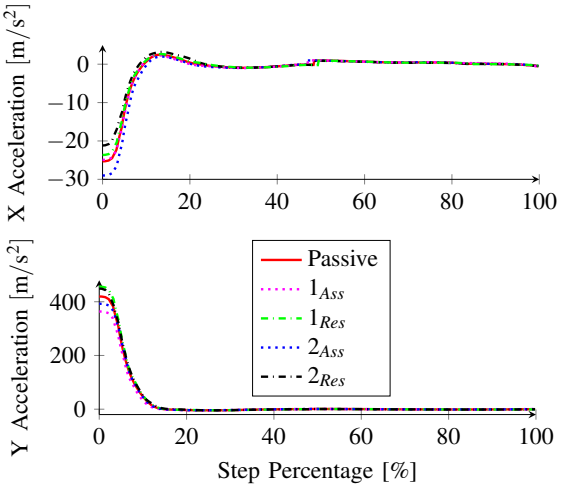

Fig. 6. The acceleration of the center of mass (COM) along horizontal and vertical directions during one steady step.

strategies, where the first type had the mass/inertia matrix multiplied by the scaling factor. The second type included additional term on the actuated part of the mass/inertia matrix to dissipate energy near the beginning and at the end of each step. Simulation results showed that the second type of strategy was able to enlarge the feasible range of the scaling factor to obtain a steady limit cycle. The second strategy also enhanced the effect of the scaling factor and provided greater assistance/resistance to the human model than the first strategy. Future work will implement these control strategies in exoskeleton hardware for pre-clinical testing with human subjects.

REFERENCES

[1] K. Suzuki, G. Mito, H. Kawamoto, Y. Hasegawa, and Y. Sankai, "Intention-based walking support for paraplegia patients with robot suit hal," *Advanced Robotics*, vol. 21, no. 12, pp. 1441–1469, 2007.

[2] G. Zeilig, H. Weingarden, M. Zwecker, I. Dudkiewicz, A. Bloch, and A. Esquenazi, "Safety and tolerance of the rewalk™ exoskeleton suit for ambulation by people with complete spinal cord injury: a pilot study," *The journal of spinal cord medicine*, vol. 35, no. 2, pp. 96–101, 2012.

[3] S. A. Kolakowsky-Hayner, J. Crew, S. Moran, and A. Shah, "Safety and feasibility of using the eksotm bionic exoskeleton to aid ambulation after spinal cord injury," *J Spine*, vol. 4, p. 003, 2013.

[4] A. Agrawal, O. Harib, A. Hereid, S. Finet, M. Masselin, L. Praly, A. D. Ames, K. Sreenath, and J. W. Grizzle, "First steps towards translating hzd control of bipedal robots to decentralized control of exoskeletons," *IEEE Access*, vol. 5, pp. 9919–9934, 2017.

[5] G. Lv and R. D. Gregg, "Underactuated potential energy shaping with contact constraints: Application to a powered knee-ankle orthosis," *IEEE Transactions on Control Systems Technology*, vol. 26, no. 1, pp. 181–193, 2018.

[6] ——, "Towards total energy shaping control of lower-limb exoskeletons," in *American Control Conference (ACC), 2017*. IEEE, 2017, pp. 4851–4857.

[7] G. Lv, H. Zhu, and R. D. Gregg, "On the design and control of highly backdrivable lower-limb exoskeletons: A discussion of past and ongoing work," *IEEE Control Systems Magazine*, vol. 38, no. 6, pp. 88–113, 2018.

[8] R. Ortega, J. A. L. Perez, P. J. Nicklasson, and H. J. Sira-Ramirez, *Passivity-based control of Euler-Lagrange systems: mechanical, electrical and electromechanical applications*. Springer Science & Business Media, 2013.

[9] A. M. Bloch, N. E. Leonard, and J. E. Marsden, "Stabilization of mechanical systems using controlled lagrangians," in *Decision and Control, 1997., Proceedings of the 36th IEEE Conference on*, vol. 3. IEEE, 1997, pp. 2356–2361.

[10] M. W. Spong, "The passivity paradigm in the control of bipedal robots," in *International Conference on Climbing and Walking Robots*. Springer, 2005, pp. 775–786.

[11] D. Auckly, L. Kapitanski, and W. White, "Control of nonlinear underactuated systems," *Communications on Pure and Applied Mathematics: A Journal Issued by the Courant Institute of Mathematical Sciences*, vol. 53, no. 3, pp. 354–369, 2000.

[12] G. Blankenstein, R. Ortega, and A. J. Van Der Schaft, "The matching conditions of controlled lagrangians and ida-passivity based control," *International Journal of Control*, vol. 75, no. 9, pp. 645–665, 2002.

[13] J. K. Holm and M. W. Spong, "Kinetic energy shaping for gait regulation of underactuated bipeds," in *2008 IEEE International Conference on Control Applications*. IEEE, 2008, pp. 1232–1238.

[14] R. M. Murray, *A mathematical introduction to robotic manipulation*. CRC press, 2017.

[15] D. Auckly and L. Kapitanski, "Mathematical problems in the control of underactuated systems," *Nonlinear Dynamics and Renormalization Group*, no. 27, pp. 29–40, 2001.

[16] R. D. Gregg and M. W. Spong, "Reduction-based control of three-dimensional bipedal walking robots," *The International Journal of Robotics Research*, vol. 29, no. 6, pp. 680–702, 2010.

[17] M. R. Yeatman, G. Lv, and R. D. Gregg, "Passivity-based control with a generalized energy storage function for robust walking of biped robots," in *American Control Conference (ACC), 2018*. IEEE, 2018.

[18] H. Zhu, J. Doan, C. Stence, G. Lv, T. Elery, and R. Gregg, "Design and validation of a torque dense, highly backdrivable powered knee-ankle orthosis," in *Robotics and Automation (ICRA), 2017 IEEE International Conference on*. IEEE, 2017, pp. 504–510.

[19] R. D. Gregg, T. Lenzi, L. J. Hargrove, and J. W. Sensinger, "Virtual constraint control of a powered prosthetic leg: From simulation to experiments with transfemoral amputees," *IEEE Transactions on Robotics*, vol. 30, no. 6, pp. 1455–1471, 2014.

[20] S. Boyd and L. Vandenberghe, *Convex optimization*. Cambridge university press, 2004.

[21] D. J. Braun, J. E. Mitchell, and M. Goldfarb, "Actuated dynamic walking in a seven-link biped robot," *IEEE/ASME Transactions on Mechatronics*, vol. 17, no. 1, pp. 147–156, 2012.

[22] J. K. Holm, "Gait regulation for bipedal locomotion," Ph.D. dissertation, University of Illinois at Urbana-Champaign, 2008.

[23] K. R. Embry, D. J. Villarreal, R. L. Macaluso, and R. D. Gregg, "Modeling the kinematics of human locomotion over continuously varying speeds and inclines," *IEEE transactions on neural systems and rehabilitation engineering*, vol. 26, no. 12, pp. 2342–2350, 2018.

[24] A. E. Martin and J. P. Schmiedeler, "Predicting human walking gaits with a simple planar model," *Journal of biomechanics*, vol. 47, no. 6, pp. 1416–1421, 2014.

[25] G. Cavagna, P. Willems, and N. Heglund, "The role of gravity in human walking: pendular energy exchange, external work and optimal speed," *The Journal of Physiology*, vol. 528, no. 3, pp. 657–668, 2000.

[26] G. Cavagna, F. Saibene, and R. Margaria, "External work in walking," *Journal of applied physiology*, vol. 18, no. 1, pp. 1–9, 1963.

[27] A. M. Bloch, N. E. Leonard, and J. E. Marsden, "Controlled lagrangians and the stabilization of mechanical systems. i. the first matching theorem," *IEEE Transactions on automatic control*, vol. 45, no. 12, pp. 2253–2270, 2000.

[28] A. M. Bloch, D. E. Chang, N. E. Leonard, and J. E. Marsden, "Controlled lagrangians and the stabilization of mechanical systems. ii. potential shaping," *IEEE Transactions on Automatic Control*, vol. 46, no. 10, pp. 1556–1571, 2001.

[29] V. T. Inman, H. D. Eberhart, *et al.*, "The major determinants in normal and pathological gait," *Journal of Bone and Joint Surgery*, vol. 35, no. 3, pp. 543–558, 1953.

[30] A. Grabowski, C. T. Farley, and R. Kram, "Independent metabolic costs of supporting body weight and accelerating body mass during walking," *Journal of Applied Physiology*, vol. 98, no. 2, pp. 579–583, 2005.